

Holographic complexity of anisotropic black branes

Seyed Ali Hosseini Mansoori^{a,c}, Viktor Jahnke^d, Mohammad M. Qaemmaqami^b and Yaithd D. Olivas^d

^a*School of Astronomy, ^b School of Particles and Accelerators
Institute for Research in Fundamental Sciences (IPM), P.O. Box 19395-5531, Tehran, Iran*

^c*Physics Department, Shahrood University of Technology,
P.O.Box 3619995161, Shahrood, Iran*

^d*Departamento de Física de Altas Energías, Instituto de Ciencias Nucleares, Universidad
Nacional Autónoma de México
Apartado Postal 70-543, CDMX 04510, México*

{shosseini, m.qaemmaqami}@ipm.ir,
{viktor.jahnke, yaithd.olivas}@correo.nucleares.unam.mx

Abstract

We use the complexity = action (CA) conjecture to study the full-time dependence of holographic complexity in anisotropic black branes. We find that the time behaviour of holographic complexity of anisotropic systems shares a lot of similarities with the behaviour observed in isotropic systems. In particular, the holographic complexity remains constant for some initial period, and then it starts to change so that the complexity growth rate violates the Lloyd's bound at initial times, and approaches this bound from above at later times. Compared with isotropic systems at the same temperature, the anisotropy reduces the initial period in which the complexity is constant and increases the rate of change of complexity. At late times the difference between the isotropic and anisotropic results is proportional to the pressure difference in the transverse and longitudinal directions.

Contents

1	Introduction	2
2	Gravity set-up	4
3	Holographic Complexity	6
3.1	Behaviour at initial times: $0 \leq t \leq t_c$	10
3.2	Behaviour at later times: $t > t_c$	12
3.2.1	Late time behaviour	15
3.2.2	Full time behaviour	16

4	Discussion	17
A	Joint terms at the $r = r_{\max}$ and $r = \epsilon_0$ cutoff surfaces	19
B	Comparison with Brown et al	20

1 Introduction

The gauge-gravity duality [1] provides a framework in which one can study the emergence of gravity from non-gravitational degrees of freedom. Within this framework, the gravitational theory lives in a higher dimensional space \mathcal{M} , usually called bulk, and the non-gravitational theory can be thought of as living on the boundary of \mathcal{M} . Despite the existence of a dictionary [2,3] relating bulk and boundary quantities, the description of the black hole’s interior in terms of boundary degrees of freedom remains elusive. Recently, there has been progress in this direction, with the conjecture that the growth of the interior of a black hole is related to the quantum computational complexity¹ of the states in the boundary theory. There are two main proposals relating the complexity to geometric quantities in the bulk, namely, the Complexity = Volume (CV) [4,5] and the Complexity = Action (CA) [6,7] conjectures. In the CV conjecture, the complexity is dual to the volume of a certain extremal surface in the bulk and provides an example of the recent proposal about connection between tensor network and geometry [8–10], while in the CA conjecture the complexity is dual to the gravitational action evaluated in certain region in the bulk. More details about CA conjecture will be given in section 3.

A convenient gravity set-up to study complexity growth is a two-sided black hole geometry. This geometry has two asymptotic regions, which we call left (L) and right (R) boundaries, and an Einstein-Rosen Bridge (ERB) connecting the two sides of the geometry. The Penrose diagram of this geometry is shown in figure 1. From the point of view of the boundary theory, the two-sided black hole is dual to a thermofield double (TFD) state, constructed out of two copies of the boundary theory [12]

$$|TFD(t_L, t_R)\rangle = \frac{1}{Z^{1/2}} \sum_n e^{\frac{-\beta E_n}{2}} e^{-iE_n(t_L+t_R)} |E_n\rangle_L |E_n\rangle_R, \quad (1)$$

where L and R label the quantum states of the left and right boundary theories, respectively. The TFD state is invariant under evolution with a Hamiltonian of the form $H = H_L - H_R$, which means that the system is invariant under the shifts $t_L \rightarrow t_L + \Delta t$, and $t_R \rightarrow t_R - \Delta t$. As a result, the TFD state only depends on the sum of the left and right boundary times $t = t_L + t_R$.

¹The quantum computational complexity is a state-dependent quantity that measures how difficult is to prepare a given state. More precisely, one starts from some reference state and defines the complexity of the target state as the minimal number of simple unitary operations required to prepare it. For a more precise definition, see the review [11].

The ERB connecting the two sides of the geometry grows linearly with time. Classically, this behaviour goes on forever. In [4] Susskind proposed that this behaviour is dual to the growth of the computational complexity in the boundary theory, which is known to persist for very long times. Using the CV proposal, the authors of [5] showed that the late-time behaviour of rate of change of holographic complexity is given by $d\mathcal{C}_V/dt = 8\pi M/(d-1)$, where M is the black hole's mass and d is the number of dimensions of the boundary theory. Despite having a qualitative agreement with the behaviour of complexity for quantum systems, the CV conjecture is defined in terms of an arbitrary length scale, which is usually taken to be of the order of the AdS length scale. In order to avoid the ambiguity associated to the arbitrary length scale the authors of [6, 7] proposed the CA conjecture. For neutral black holes, the late time behaviour of the rate of change of holographic complexity reaches a constant value which is also proportional to the black hole's mass

$$\lim_{t \rightarrow \infty} \frac{d\mathcal{C}_A}{dt} = \frac{2M}{\hbar\pi} . \quad (2)$$

This late-time behaviour may be associated with the Lloyd's bound on the rate of computation by a system with energy M [13]. This saturation of the complexification bound lead to the conjecture that the black holes are the fastest computers in nature [7]. It was later shown that a more precise definition of \mathcal{C}_A requires the introduction of joint and boundary terms, which were not present in the calculation of [6, 7]. In particular, it was shown that the CA proposal also have an ambiguity related to the parametrization of null surfaces [14]. Using the boundary and joint terms derived in [14, 15], the authors of [16, 17] showed that these ambiguities do not affect the late time behaviour of $d\mathcal{C}_A/dt$, but they play a role at early times, leading to a violation of Lloyd's bound.

Therefore, both the CA and the CV proposals have ambiguities which (apparently) cannot be eliminated. This is not a problem, however, because the same ambiguities were found in the definition of complexity for free quantum field theories [18, 19]. Moreover, the quantitative disagreement between the results obtained with the CA and CV proposals might be related to other ambiguities in the definition of complexity, like the choice of the reference state or the choice of the elementary gates.

The Lloyd's bound was shown to be violated even at late times by anisotropic systems, including the SYM theory defined in a non-commutative geometry [20], and Lifshitz and hyperscaling violating geometries [21–23]. This raises the question of whether there is a more general bound that is also respected by anisotropic systems. With this in mind, in this paper we use the CA conjecture to study the holographic complexity of a class of anisotropic black branes². We consider the solution of Mateos and Trancanelli (MT) [24, 25] and study the time dependence of holographic complexity in thermofield double states which are dual to two-sided black brane geometries. This model is a solution of type IIB supergravity that was designed to model the effects of anisotropy in the quark-gluon plasma (QGP) created in heavy ion collisions. The anisotropy is present in the initial stages after the collision and it leads to different transverse and longitudinal pressures in the plasma. For our purposes,

²Some previous work on holographic complexity include, for instance, [26–63].

the main motivation to consider this model is that it describes a renormalization group (RG) flow from an AdS geometry in the ultraviolet (UV) to a Lifshitz-like geometry in the infrared (IR). The transition is controlled by the ratio a/T , where a is a parameter that measures the degree of anisotropy and T is the black brane's temperature. This parameter is small close to the UV fixed point and large close the IR fixed point. We would like to understand how the complexity rate changes as we move along this RG flow and whether this system respects the Lloyd's bound. For technical convenience, we have only considered small deviations from the UV fixed point, i.e., small values of a/T , which can be incorporated by considering an analytical black brane solution with small corrections due to anisotropy³.

We find that the time behaviour of holographic complexity is qualitatively similar to the behaviour observed for isotropic systems, namely, the holographic complexity remains constant for some period, and then it starts to change so that the rate of complexity growth violates the Lloyd's bound at initial times, and it approaches this bound from above at later times. Additionally, we find that the net effect of anisotropy is basically a vertical upward shift in the curves of the rate of change of holographic complexity versus time. At later times, the difference between the isotropic and anisotropic results is proportional to the difference in pressures in the longitudinal and transverse directions.

The remainder of paper is organized as follows. In section 2 we review the anisotropic black brane solution of Mateos and Trancanelli and present some of its thermodynamic properties. In section 3 we use the CA conjecture to study the full-time behaviour of holographic complexity of thermofield double states which are dual to two-sided anisotropic black branes solutions of Mateos and Trancanelli. We discuss our results in section 4. We relegate to two appendices some technical details of the calculations.

2 Gravity set-up

Anisotropic black branes: the MT model

The Mateos and Trancanelli (MT) model [24,25] is a solution of type IIB supergravity whose effective action in five dimensions can be written as

$$S = \frac{1}{16\pi G_N} \int_{\mathcal{M}} d^5x \sqrt{-g} \left[R + \frac{12}{L^2} - \frac{1}{2} (\partial\phi)^2 - \frac{1}{2} e^{2\phi} (\partial\chi)^2 \right] + S_{\text{GH}}, \quad (3)$$

where ϕ , χ and $g_{\mu\nu}$ are the dilaton field, the axion field and the metric respectively, G_N is the five-dimensional Newton constant, and S_{GH} is the Gibbons-Hawking term. The solution in Einstein frame takes the form

$$ds^2 = L^2 e^{-\phi(r)/2} \left[-r^2 \mathcal{F}(r) \mathcal{B}(r) dt^2 + \frac{dr^2}{r^2 \mathcal{F}(r)} + r^2 (dx^2 + dy^2 + \mathcal{H}(r) dz^2) \right] \quad (4)$$

$$\chi = a z, \quad \phi = \phi(r), \quad \mathcal{H} = e^{-\phi}, \quad (5)$$

³To investigate the entire RG flow it is necessary to consider arbitrary values of a/T . This leads to technical difficulties because the solution needs to be calculated numerically in these cases.

where (t, x, y, z) are the gauge theory coordinates and r is the AdS radial coordinate. Here L is the AdS radius, which we set to unity in the following⁴. The above solution has a horizon at $r = r_{\text{H}}$ and the boundary is located at $r = \infty$, where $\mathcal{F} = \mathcal{B} = \mathcal{H} = 1$ and $\phi = 0$. The axion is proportional to the z -coordinate and this introduces an anisotropy into the system, which is measured by the anisotropy parameter a . For $a \neq 0$, the above solution corresponds to the gravity dual of $\mathcal{N} = 4$ SYM theory, with gauge group $SU(N)$, deformed by a position-dependent theta term. When $a = 0$, the above solution reduces to the gravity dual of the undeformed SYM theory. The functions \mathcal{F} , \mathcal{B} , \mathcal{H} and the dilaton ϕ can be determined analytically⁵ for small values of the anisotropy parameter a as

$$\begin{aligned}\mathcal{F} &= 1 - \frac{r_{\text{H}}^4}{r^4} + \frac{a^2}{24r^4r_{\text{H}}^2} \left[8r^2r_{\text{H}}^2 - 2r_{\text{H}}^2(4 + 5\log 2) + (3r^4 + 7r_{\text{H}}^4) \log \left(1 + \frac{r_{\text{H}}^2}{r^2} \right) \right], \\ \mathcal{B} &= 1 - \frac{a^2}{24r_{\text{H}}^2} \left[\frac{10r_{\text{H}}^2}{r^2 + r_{\text{H}}^2} + \log \left(1 + \frac{r_{\text{H}}^2}{r^2} \right) \right], \\ \phi &= -\frac{a^2}{4r_{\text{H}}^2} \log \left(1 + \frac{r_{\text{H}}^2}{r^2} \right)\end{aligned}\tag{6}$$

By requiring regularity of the Euclidean continuation of the above metric at the horizon, one obtains the Hawking temperature as

$$T = \frac{r_{\text{H}}}{\pi} + \frac{(5\log 2 - 2)a^2}{48\pi r_{\text{H}}}\tag{7}$$

The Bekenstein-Hawking entropy can be obtained from the horizon area as

$$S = \frac{r_{\text{H}}^3}{4G_{\text{N}}} \left(1 + \frac{5a^2}{16r_{\text{H}}^2} \right) V_3\tag{8}$$

where $V_3 = \int dx dy dz$ is the volume in the xyz -directions. Using holographic renormalization the stress tensor of the deformed SYM theory can be obtained as [25, 66]

$$T_{ij} = \text{diag}(E, P_{xy}, P_{xy}, P_z),\tag{9}$$

where

$$E = \frac{3\pi^2 N^2 T^4}{8} + \frac{N^2 T^2}{32} a^2,\tag{10}$$

is the energy density of the black brane and

$$P_{xy} = \frac{\pi^2 N^2 T^4}{8} + \frac{N^2 T^2}{32} a^2, \quad P_z = \frac{\pi^2 N^2 T^4}{8} - \frac{N^2 T^2}{32} a^2,\tag{11}$$

⁴Note that $L = 1$ implies that $G_{\text{N}} = \frac{\pi}{2N^2}$ (see e.g. [64]), where N is the rank of the gauge group $SU(N)$ of the dual field theory.

⁵For generic values of the anisotropy parameter, the metric functions can be determined numerically. For more details, see the appendix A of [25].

are the pressures along the transverse and longitudinal directions, respectively. The mass of the black brane can then be calculated as

$$M = E V_3 = \left(\frac{3\pi^2 N^2 T^4}{8} + \frac{N^2 T^2}{32} a^2 \right) V_3, \quad (12)$$

A more simple way of calculating the black brane's mass is through the expression

$$M = \int T dS = \int_0^{r_H} T(r_H) \frac{dS(r_H)}{dr_H} dr_H = \frac{V_3}{16\pi G_N} \left[3r_H^4 + \frac{r_H^2 a^2}{4} (5 \log 2 - 1) \right]. \quad (13)$$

where the integral was calculated using the equations (7) and (8) for $T(r_H)$ and $S(r_H)$, respectively. Expressing r_H as a function of the temperature T and using that $G_N = \pi/(2N^2)$, we recover the expression for the mass given in equation (12).

Note that the mass of the anisotropic black brane is larger than the mass of an isotropic black brane with the same temperature, or with the same horizon radius. For future reference, we note that

$$M(a) = M(0) + \frac{V_3}{2} (P_{xy} - P_z). \quad (14)$$

Lastly, we comment that the above gravitational solution can be extended to a two-sided eternal black brane geometry, with two asymptotic boundaries. See figure 1. The extended solution is dual to a thermofield double state constructed out of two copies of the boundary theory.

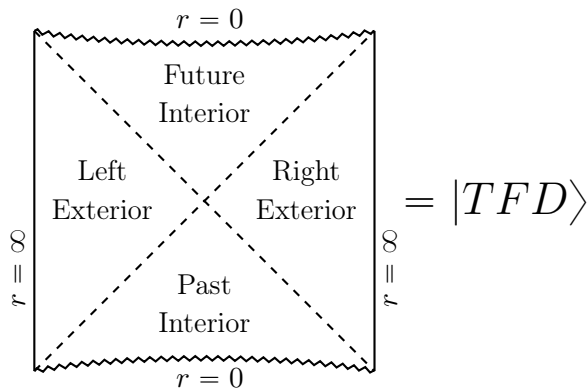


Figure 1: Penrose diagram for the two-sided black branes we consider. This geometry is dual to a thermofield double state constructed out of two copies of the boundary theory.

3 Holographic Complexity

In this section we compute the holographic complexity using the complexity=action (CA) [6, 7]. Here we follow closely the analysis of [16], with small adaptations for anisotropic systems. We consider neutral anisotropic black branes with a generic bulk action of the form

$$S = \frac{1}{16\pi G_N} \int d^d x dr \mathcal{L}(r, x), \quad (15)$$

and metric

$$ds^2 = -G_{tt}(r)dt^2 + G_{rr}(r)dr^2 + G_{ij}(r)dx^i dx^j, \quad i, j = 1, 2, \dots, d-1, \quad (16)$$

where r is the AdS radial coordinate and (t, x^i) are the gauge theory coordinates. We take the boundary as located at $r = \infty$ and we assume the existence of a horizon at $r = r_H$, where G_{tt} has a zero and G_{rr} has a simple pole. We denote as G the determinant of G_{ij} , i.e. $G = \det(G_{ij})$.

In the computations of holographic complexity it is convenient to use coordinates that cover smoothly the two sides of the geometry. We use Eddington-Finkelstein coordinates

$$u = t - r^*(r), \quad v = t + r^*(r), \quad (17)$$

where the tortoise coordinate is defined as

$$r^*(r) = \text{sgn}(G_{tt}(r)) \int^r dr' \sqrt{\frac{G_{rr}(r')}{G_{tt}(r')}}. \quad (18)$$

The CA conjecture states that the quantum complexity of the state of the boundary theory is given by the gravitational action evaluated in a region of the bulk known as the Wheeler-DeWitt (WDW) patch

$$\mathcal{C}_A = \frac{I_{\text{WDW}}}{\pi \hbar} \quad (19)$$

The WDW patch is the domain of dependence of any spatial slice anchored at a given pair of boundary times (t_L, t_R) . See figure 2. The gravitational action in the WDW patch is divergent because this region extends all the way up to the asymptotic boundaries of the space-time. We regularize this divergence by introducing a cutoff surface at $r = r_{\text{max}}$ near the boundaries. We also introduce a cutoff surface $r = \epsilon_0$ near to the past and future singularities. Without loss of generality, we consider the time evolution of holographic complexity for the symmetric configuration $t_L = t_R = t/2$. More general cases can be obtained from the symmetric configuration by using the fact that the system is symmetric under shifts $t_L \rightarrow t_L + \Delta t$ and $t_R \rightarrow t_R - \Delta t$.

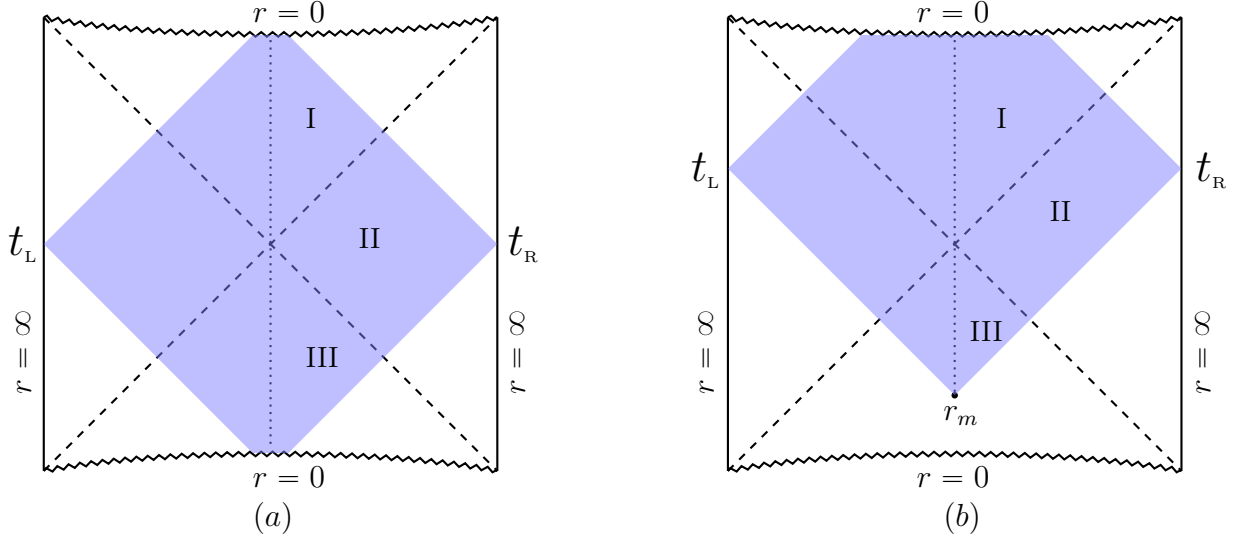


Figure 2: Penrose diagram and the WDW patch (blue region) for the two-sided black brane we consider. (a) Configuration at initial times ($t \leq t_c$) in which the WDW patch intersects both the future and the past singularity. (b) Configuration at later times ($t > t_c$) when the WDW patch no longer intersects the past singularity.

The gravitational action in the WDW patch can be written as

$$I_{\text{WDW}} = I_{\text{bulk}} + I_{\text{surface}} + I_{\text{joint}}, \quad (20)$$

where

$$I_{\text{bulk}} = \frac{1}{16\pi G_N} \int_{\mathcal{M}} d^{d+1}x \sqrt{-g} \mathcal{L}(x) \quad (21)$$

is the bulk action and I_{surface} and I_{joint} are surface and joint terms that are necessary to have a well-defined variational principle when one considers a finite domain of space-time [14]. The surface terms are given by

$$I_{\text{surface}} = \frac{1}{8\pi G_N} \int_{\mathcal{B}} d^d x \sqrt{|h|} K \pm \frac{1}{8\pi G_N} \int_{\mathcal{B}'} d\lambda d^{d-1} \theta \sqrt{\gamma} \kappa \quad (22)$$

where the first term, which is defined in terms of the trace of the extrinsic curvature K , is the well-known Gibbons-Hawking-York boundary term [67, 68]. This term is necessary when the boundary includes (smooth) space-like and time-like segments, which we denoted as \mathcal{B} . The second term in the above equation includes the contribution of null segments. This term is defined in terms of the parameter κ , which measure how much the null surface \mathcal{B}' fails to be affinely parametrized. Here we follow [14] and set $\kappa = 0$, so that we do not need to consider these null boundary terms. This choice of κ correspond to affinely parametrize the null boundary surfaces.

The joint terms are necessary when the intersection of two boundary terms is not smooth. These terms can be written as

$$I_{\text{joint}} = \frac{1}{8\pi G_N} \int_{\pm} d^{d-1}x \sqrt{\sigma} \eta + \frac{1}{8\pi G_N} \int_{\pm'} d^{d-1}x \sqrt{\sigma} a \quad (23)$$

where the first term⁶ corresponds to the intersection of two boundary segments which can be time-like or space-like, so the intersection can be of the type: time-like/time-like, time-like/space-like or space-like/space-like. As the WDW patch do not include such intersection, we do not need to consider this first term. The second term includes the contribution of the intersection of a null segment with any other boundary segment, so it includes contribution of the type: null/null, null/time-like and null/space-like. A more precise definition of the surface and joint terms will be given throughout the text along with the adopted conventions⁷.

As first pointed out in [19], at early times the WDW patch intersects both the future and the past singularity, and this causes I_{WDW} to be constant for some period of time $0 \leq t \leq t_c$. At later times, $t > t_c$, the WDW patch no longer intersects the past singularity, and I_{WDW} starts to change with time. These two cases are illustrated in figure 2. The time scales separating these two regimes can be written as

$$t_c = 2 (r_\infty^* - r^*(0)) , \quad r_\infty^* = \lim_{r \rightarrow \infty} r^*(r) \quad (24)$$

where we have used that $t_L = t_R = t/2$.

Figure 3 shows how the critical time (24) behaves as a function of the anisotropy parameter in MT model. This figure shows that, as compared to an isotropic system at the same temperature, the anisotropy reduces the critical time, i.e., the complexity starts to change earlier in anisotropic systems.

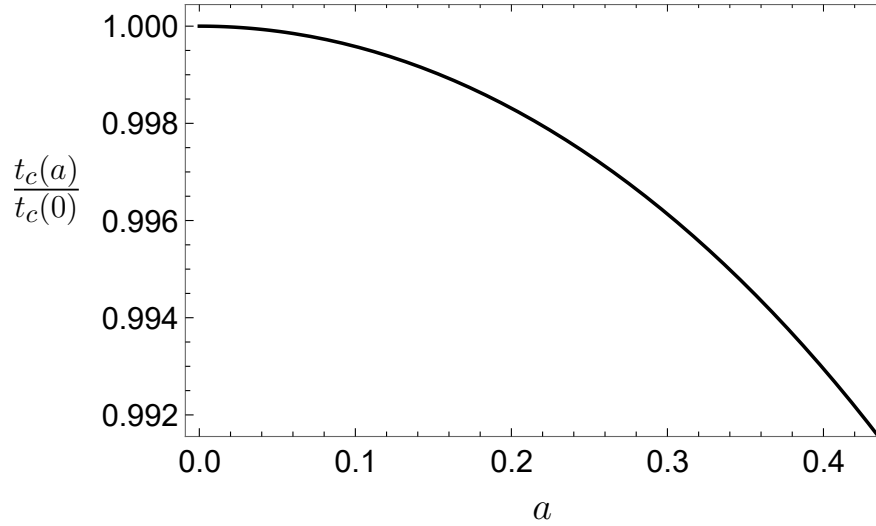


Figure 3: Critical time (normalized by isotropic result) versus the anisotropy parameter a . Here we have fixed the temperature $T = 1/\pi$.

⁶This contribution is known as the Hayward joint term [69, 70].

⁷Here we adopted the conventions found in the appendix A of [15].

3.1 Behaviour at initial times: $0 \leq t \leq t_c$

For initial times $0 \leq t \leq t_c$ the WDW patch intersects with both the future and past singularities. The contributions for I_{WDW} include: the bulk term, the GHY terms and the joint terms. In principle, the GHY terms include contributions from the cutoff surfaces at $r = r_{\text{max}}$ and $r = \epsilon_0$, as well as from the null boundaries of the WDW patch. However, since we affinely parametrize the null surfaces, we do not need to consider the surface contributions from the null boundaries. The joint terms include contribution from the intersection of the null boundaries of the WDW patch with the cutoff surfaces at $r = r_{\text{max}}$ and $r = \epsilon_0$. We use the left-right symmetry of the WDW patch to calculate I_{WDW} for the right side of Penrose diagram and then multiply the result by two.

To calculate the bulk contributions we split the right-side of the WDW patch into three parts: region I, region II and region III, which are shown in figure 2 (a). We then calculate the bulk contribution as

$$I_{\text{bulk}}(t \leq t_c) = 2(I_{\text{bulk}}^{\text{I}} + I_{\text{bulk}}^{\text{II}} + I_{\text{bulk}}^{\text{III}}), \quad (25)$$

where⁸

$$I_{\text{bulk}}^{\text{I}} = \frac{V_{d-1}}{16\pi G_{\text{N}}} \int_{\epsilon_0}^{r_{\text{H}}} dr \sqrt{G_{tt} G_{rr} G} \mathcal{L}(r) \left(\frac{t}{2} + r_{\infty}^* - r^*(r) \right) \quad (26)$$

$$I_{\text{bulk}}^{\text{II}} = \frac{V_{d-1}}{8\pi G_{\text{N}}} \int_{r_{\text{H}}}^{r_{\text{max}}} dr \sqrt{G_{tt} G_{rr} G} \mathcal{L}(r) (r_{\infty}^* - r^*(r)) \quad (27)$$

$$I_{\text{bulk}}^{\text{III}} = \frac{V_{d-1}}{16\pi G_{\text{N}}} \int_{\epsilon_0}^{r_{\text{H}}} dr \sqrt{G_{tt} G_{rr} G} \mathcal{L}(r) \left(-\frac{t}{2} + r_{\infty}^* - r^*(r) \right) \quad (28)$$

with $G = \det(G_{ij})$ and $V_{d-1} = \int d^{d-1}x$. Note that in the above expressions we are assuming that the on-shell Lagrangian \mathcal{L} only depends on r . Summing all the contributions we obtain

$$I_{\text{bulk}}(t \leq t_c) = \frac{1}{4\pi G_{\text{N}}} \int_{\epsilon_0}^{r_{\text{max}}} dr \sqrt{G_{tt} G_{rr} G} \mathcal{L}(r) (r_{\infty}^* - r^*(r)). \quad (29)$$

Note that $I_{\text{bulk}}(t \leq t_c)$ does not depend on time.

Now we turn to the computation of the GHY surface terms. These contribution come from the cutoff surfaces at $r = r_{\text{max}}$ on the two sides of the geometry and from the cutoff surfaces at $r = \epsilon_0$ both at the past and future singularities. In either cases the surfaces are described by a relation of the form $r = \text{constant}$, and the outward-directed normal vector are proportional to $\partial_{\mu}(r - \text{constant})$. We write the corresponding normal as

$$n_{\mu} = (n_t, n_r, n_i) = b(0, 1, 0), \quad (30)$$

⁸Here we are using that $I_{\text{bulk}}^{\text{I}} = \frac{1}{16\pi G_{\text{N}}} \int_I d^{d+1}x \sqrt{-g} \mathcal{L}(x) = \frac{1}{16\pi G_{\text{N}}} \int_I d^{d-1}x \int dr \sqrt{G_{tt} G_{rr} G} \mathcal{L}(R) \int_0^{v_1 - r^*(r)} dt$, where $v_1 = t_R + r_{\infty}^*$ defines the future null boundary of the right side of the WDW patch. In region II, for instance, the integral over the time coordinate is $\int_{u_1 + r^*(r)}^{v_1 - r^*(r)} dt = 2(r_{\infty}^* - r^*(r))$, where $u_1 = t_R - r_{\infty}^*$ defines the past null boundary of the right side of the WDW patch.

where b is some normalization constant. We normalize the normal vector as $n^2 = n^r n_r = \pm 1$, where the plus sign is for space-like vectors at the $r = r_{\max}$ cutoff surface, and the minus sign if for the time-like vectors at the $r = \epsilon_0$ cutoff surface. We obtain

$$n_\mu^{(s)} = (n_t^{(s)}, n_r^{(s)}, n_i^{(s)}) = (0, \sqrt{G_{rr}(r_{\max})}, 0), \quad \text{at } r = r_{\max}, \quad (31)$$

$$n_\mu^{(t)} = (n_t^{(t)}, n_r^{(t)}, n_i^{(t)}) = (0, \sqrt{-G_{rr}(\epsilon_0)}, 0), \quad \text{at } r = \epsilon_0. \quad (32)$$

where the superscript (s) denotes space-like vectors, while the superscript (t) denotes time-like vectors. The trace of the extrinsic curvature of these r -constant surfaces can be calculated as

$$\begin{aligned} K &= \nabla_\mu n^\mu = \frac{1}{\sqrt{-g}} \partial_r (\sqrt{-g} n^r) \Big|_{r=\epsilon_0, r_{\max}} \\ &= \frac{1}{2\sqrt{\mp G_{rr}}} \left[\frac{\partial_r G_{tt}}{G_{tt}} + \frac{\partial_r G}{G} \right] \Big|_{r=\epsilon_0, r_{\max}} \end{aligned} \quad (33)$$

where we use the minus sign for the $r = \epsilon_0$ surface and the plus sign for the $r = r_{\max}$ surface.

The GHY surface contributions can then be written as

$$I_{\text{surface}}(t \leq t_c) = I_{\text{surface}}^{\text{future}} + I_{\text{surface}}^{\text{past}} + I_{\text{surface}}^{\text{bdry}} \quad (34)$$

where the contributions from the cutoff surfaces at future and past singularities are given by

$$\begin{aligned} I_{\text{surface}}^{\text{future}} &= \frac{V_{d-1}}{8\pi G_N} \sqrt{\frac{G_{tt}G}{G_{rr}}} \left[\frac{\partial_r G_{tt}}{G_{tt}} + \frac{\partial_r G}{G} \right] \left(\frac{t}{2} + r_\infty^* - r^*(r) \right) \Big|_{r=\epsilon_0}, \\ I_{\text{surface}}^{\text{past}} &= \frac{V_{d-1}}{8\pi G_N} \sqrt{\frac{G_{tt}G}{G_{rr}}} \left[\frac{\partial_r G_{tt}}{G_{tt}} + \frac{\partial_r G}{G} \right] \left(-\frac{t}{2} + r_\infty^* - r^*(r) \right) \Big|_{r=\epsilon_0}, \end{aligned} \quad (35)$$

and the contributions from the cutoff surfaces at the two asymptotic boundaries read

$$I_{\text{surface}}^{\text{bdry}} = \frac{V_{d-1}}{8\pi G_N} \sqrt{\frac{G_{tt}G}{G_{rr}}} \left[\frac{\partial_r G_{tt}}{G_{tt}} + \frac{\partial_r G}{G} \right] (r_\infty^* - r^*(r)) \Big|_{r=r_{\max}}. \quad (36)$$

In the above expressions we have already multiplied the results by two to account for the two sides of the WDW patch. Note that $I_{\text{surface}}^{\text{bdry}}$ does not depend on time. Moreover, the time dependence of $I_{\text{surface}}^{\text{future}}$ and $I_{\text{surface}}^{\text{past}}$ cancel, so that the total surface contribution is time-independent

$$I_{\text{surface}}(t \leq t_c) = \frac{V_{d-1}}{4\pi G_N} \sqrt{\frac{G_{tt}G}{G_{rr}}} \left[\frac{\partial_r G_{tt}}{G_{tt}} + \frac{\partial_r G}{G} \right] (r_\infty^* - r^*(r)) \Big|_{r=\epsilon_0} + \quad (37)$$

$$+ \frac{V_{d-1}}{8\pi G_N} \sqrt{\frac{G_{tt}G}{G_{rr}}} \left[\frac{\partial_r G_{tt}}{G_{tt}} + \frac{\partial_r G}{G} \right] (r_\infty^* - r^*(r)) \Big|_{r=r_{\max}}. \quad (38)$$

The only terms left to calculate are the joint contributions that come from the intersections of the null boundaries of the WDW patch with the cutoff surfaces at $r = r_{\max}$ and $r = \epsilon_0$. The joint terms can be written as

$$I_{\text{joint}} = I_{\text{joint}}^{\text{sing}} + I_{\text{joint}}^{\text{bdry}}, \quad (39)$$

where $I_{\text{joint}}^{\text{sing}}$ includes the contributions from the past and future singularities and $I_{\text{joint}}^{\text{bdry}}$ corresponds to the contribution from the two asymptotic boundaries. In [30] it was shown that, for a large class of isotropic systems, the contribution from the asymptotic boundaries do not depend on time, while the contributions at $r = \epsilon_0$ vanish. We show in appendix A that this also happens in anisotropic systems. So we can write

$$I_{\text{joint}}(t \leq t_c) = I_{\text{joint}}^{\text{bdry}}. \quad (40)$$

where $I_{\text{joint}}^{\text{bdry}}$ does not depend on time.

Finally, as none of the terms I_{bulk} , I_{surface} and I_{joint} depend on time for $0 \leq t \leq t_c$, the gravitational action evaluated on the WDW patch is constant for this period of time

$$\frac{dI_{\text{WDW}}}{dt} = 0, \quad \text{for } 0 \leq t \leq t_c. \quad (41)$$

3.2 Behaviour at later times: $t > t_c$

For later times $t > t_c$ the WDW patch no longer intersects with the past singularity. In this case, there are no surface and joint terms related to the past singularity, but there is an additional joint term that comes from the intersection of two null boundaries of the WDW patch. See figure 2 (b). Again, we calculate all the contribution for the right side of the WDW patch and multiply the results by two to account for the two sides of the geometry.

To compute the bulk contribution, we again split the right side of the WDW patch into three regions, which we call I, II and III. See figure 2 (b). We write the total bulk contribution as

$$I_{\text{bulk}}(t > t_c) = 2(I_{\text{bulk}}^{\text{I}} + I_{\text{bulk}}^{\text{II}} + I_{\text{bulk}}^{\text{III}}), \quad (42)$$

where now

$$I_{\text{bulk}}^{\text{I}} = \frac{V_{d-1}}{16\pi G_N} \int_{\epsilon_0}^{r_H} dr \sqrt{G_{tt}G_{rr}G} \mathcal{L}(r) \left(\frac{t}{2} + r_\infty^* - r^*(r) \right) \quad (43)$$

$$I_{\text{bulk}}^{\text{II}} = \frac{V_{d-1}}{8\pi G_N} \int_{r_H}^{r_{\text{max}}} dr \sqrt{G_{tt}G_{rr}G} \mathcal{L}(r) (r_\infty^* - r^*(r)) \quad (44)$$

$$I_{\text{bulk}}^{\text{III}} = \frac{V_{d-1}}{16\pi G_N} \int_{r_m}^{r_H} dr \sqrt{G_{tt}G_{rr}G} \mathcal{L}(r) \left(-\frac{t}{2} + r_\infty^* - r^*(r) \right) \quad (45)$$

where the only difference from the $0 \leq t \leq t_c$ case is that the r -integral in the region III starts at the point $r = r_m$, instead of starting at the cutoff surface $r = \epsilon_0$ at the past singularity. The point r_m determines the intersection of the two past null boundaries of the WDW patch and it satisfies the equation

$$\frac{t}{2} - r_\infty^* + r^*(r_m) = 0. \quad (46)$$

which we can solve numerically. Note that we recover the equation that gives the critical time t_c when we take the limit $r_m \rightarrow 0$ in the above equation.

Summing the above contributions we can write the bulk term at later times as the bulk term at initial times plus a time-dependent term

$$I_{\text{bulk}}(t > t_c) = I_{\text{bulk}}(t \leq t_c) + \frac{V_{d-1}}{8\pi G_N} \int_{\epsilon_0}^{r_m} dr \sqrt{G_{tt} G_{rr}} G \mathcal{L}(r) \left(\frac{t}{2} - r_\infty^* + r^*(r) \right). \quad (47)$$

where $I_{\text{bulk}}(t \leq t_c)$ is given in equation (29).

For later times the GHY term includes contributions from the future singularity and from the two asymptotic boundaries. The contributions from the cutoff surfaces at the asymptotic boundaries do not depend on time, and have the same value that they have for $t \leq t_c$. The contribution from the cutoff surface at the future singularity reads

$$I_{\text{surface}}^{\text{future}} = \frac{V_{d-1}}{8\pi G_N} \sqrt{\frac{G_{tt} G}{G_{rr}}} \left[\frac{\partial_r G_{tt}}{G_{tt}} + \frac{\partial_r G}{G} \right] \left(\frac{t}{2} + r_\infty^* - r^*(r) \right) \Big|_{r=\epsilon_0}. \quad (48)$$

The total surface term can be written as

$$I_{\text{surface}}(t > t_c) = I_{\text{surface}}(t \leq t_c) + \frac{V_{d-1}}{8\pi G_N} \sqrt{\frac{G_{tt} G}{G_{rr}}} \left[\frac{\partial_r G_{tt}}{G_{tt}} + \frac{\partial_r G}{G} \right] \left(\frac{t}{2} + r_\infty^* - r^*(r) \right) \Big|_{r=\epsilon_0}. \quad (49)$$

where $I_{\text{surface}}(t \leq t_c)$ is defined in equation (38).

Finally, we turn to the computation of the joint terms. These terms include time-independent contributions from the two asymptotic boundaries, which are equal to the corresponding quantities for $t \leq t_c$, a vanishing contribution from the cutoff surface at the future singularity and a contribution from the intersection of the two null boundaries of the WDW patch. The joint term can then be written as

$$I_{\text{joint}}(t > t_c) = I_{\text{joint}}^{\text{bdry}} + I_{\text{joint}}^{\text{null}}, \quad (50)$$

where $I_{\text{joint}}^{\text{null}}$ is the contribution from the intersection of the two null boundaries. This term reads

$$I_{\text{joint}}^{\text{null}} = \frac{1}{8\pi G_N} \int d^{d-1} x \sqrt{G} a \quad (51)$$

where a is defined in terms of the left and right null vectors that parametrize the null boundaries of the WDW patch. These null vectors are given by

$$k_\mu^{\text{L}} = -\alpha \partial_\mu(t - r^*), \quad k_\mu^{\text{R}} = \alpha \partial_\mu(t + r^*) \quad (52)$$

In terms of k_μ^{L} and k_μ^{R} the quantity a can be written as

$$a = \log \left| \frac{1}{2} k^{\text{L}} \cdot k^{\text{R}} \right| = -\log \left| \frac{G_{tt}(r_m)}{\alpha^2} \right|. \quad (53)$$

Using the above expressions we can write

$$I_{\text{joint}}^{\text{null}} = -\frac{V_{d-1}}{8\pi G_N} \sqrt{G(r_m)} \log \left| \frac{G_{tt}(r_m)}{\alpha^2} \right|. \quad (54)$$

where r_m is given by equation (46). The null vectors k_μ^L and k_μ^R are defined in terms of an arbitrary normalization constant α that introduces an ambiguity in the calculation of I_{WDW} . With the above results, the joint term can be written as

$$I_{\text{joint}}(t > t_c) = I_{\text{joint}}(t \leq t_c) - \frac{V_{d-1}}{8\pi G_N} \sqrt{G(r_m)} \log \left| \frac{G_{tt}(r_m)}{\alpha^2} \right|. \quad (55)$$

Note that for $t > t_c$ the gravitational action calculated in the WDW patch can be written as

$$I_{\text{WDW}}(t > t_c) = I_{\text{WDW}}(t \leq t_c) + \delta I, \quad (56)$$

where

$$\delta I = \delta I_{\text{bulk}} + \delta I_{\text{surface}} + \delta I_{\text{joint}}, \quad (57)$$

with

$$\delta I_{\text{bulk}} = I_{\text{bulk}}(t > t_c) - I_{\text{bulk}}(t \leq t_c) = \frac{V_{d-1}}{8\pi G_N} \int_{\epsilon_0}^{r_m} dr \sqrt{G_{tt} G_{rr}} G \mathcal{L}(r) \left[\frac{\delta t}{2} + r^*(r) - r^*(0) \right], \quad (58)$$

$$\delta I_{\text{surface}} = I_{\text{surface}}(t > t_c) - I_{\text{surface}}(t \leq t_c) = \frac{V_{d-1}}{8\pi G_N} \sqrt{\frac{G_{tt} G}{G_{rr}}} \left[\frac{\partial_r G_{tt}}{G_{tt}} + \frac{\partial_r G}{G} \right] \frac{\delta t}{2} \Big|_{r=\epsilon_0}, \quad (59)$$

$$\delta I_{\text{joint}} = I_{\text{joint}}(t > t_c) - I_{\text{joint}}(t \leq t_c) = -\frac{V_{d-1}}{8\pi G_N} \sqrt{G(r_m)} \log \left| \frac{G_{tt}(r_m)}{\alpha^2} \right|. \quad (60)$$

It is convenient to work with the time variable $\delta t = t - t_c$, which is related to r_m as

$$\frac{\delta t}{2} + r^*(r_m) - r^*(0) = 0 \quad (61)$$

Finally, the time derivative of each contribution reads

$$\frac{d\delta I_{\text{bulk}}}{dt} = \frac{V_{d-1}}{16\pi G_N} \int_{\epsilon_0}^{r_m} dr \sqrt{G_{tt} G_{rr}} G \mathcal{L}(r), \quad (62)$$

$$\frac{d\delta I_{\text{surface}}}{dt} = \frac{V_{d-1}}{16\pi G_N} \sqrt{\frac{G_{tt} G}{G_{rr}}} \left(\frac{\partial_r G_{tt}}{G_{tt}} + \frac{\partial_r G}{G} \right) \Big|_{r=\epsilon_0}, \quad (63)$$

$$\frac{d\delta I_{\text{joint}}}{dt} = \frac{V_{d-1}}{16\pi G_N} \left(\frac{1}{2} \sqrt{\frac{G_{tt}}{G_{rr} G}} (\partial_r G) \log \left| \frac{G_{tt}}{\alpha^2} \right| + \sqrt{\frac{G}{G_{rr} G_{tt}}} \partial_r G_{tt} \right) \Big|_{r=r_m}. \quad (64)$$

The time derivative of I_{WDW} can then be computed as

$$\begin{aligned} \frac{dI_{\text{WDW}}}{dt} = \frac{V_{d-1}}{16\pi G_N} & \left[\int_{\epsilon_0}^{r_m} dr \sqrt{G_{tt} G_{rr}} G \mathcal{L}(r) + \sqrt{\frac{G_{tt} G}{G_{rr}}} \left(\frac{\partial_r G_{tt}}{G_{tt}} + \frac{\partial_r G}{G} \right) \Big|_{r=\epsilon_0} \right. \\ & \left. + \left(\frac{1}{2} \sqrt{\frac{G_{tt}}{G_{rr} G}} (\partial_r G) \log \left| \frac{G_{tt}}{\alpha^2} \right| + \sqrt{\frac{G}{G_{rr} G_{tt}}} \partial_r G_{tt} \right) \Big|_{r=r_m} \right] \end{aligned} \quad (65)$$

The time derivative of the holographic complexity can be obtained as

$$\frac{d\mathcal{C}_A}{dt} = \frac{1}{\pi \hbar} \frac{dI_{\text{WDW}}}{dt}. \quad (66)$$

3.2.1 Late time behaviour

In this section we now apply the formula (65) for the MT model to study the late time behaviour of the time-derivative of \mathcal{C}_A . We first observe that, at later times, r_m approaches r_H . This can be seen in figure 4, where we plot r_m versus δt .

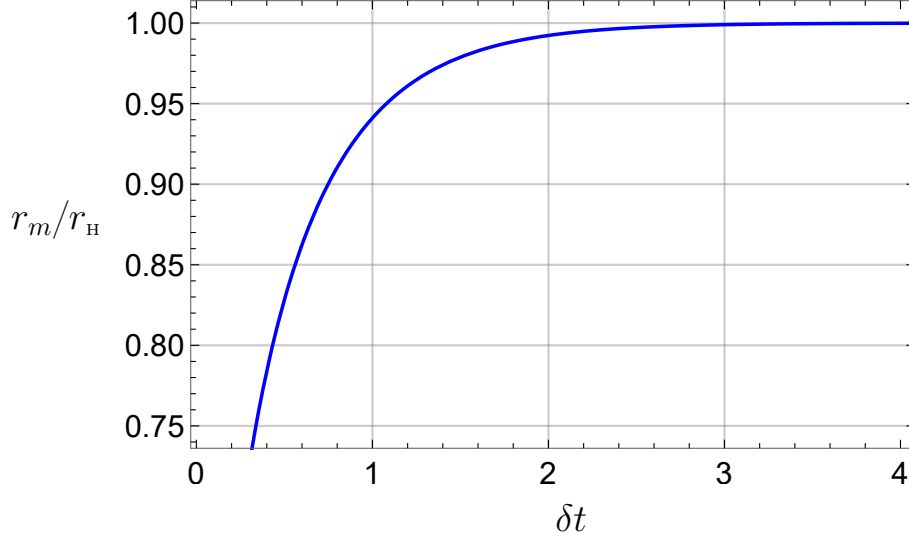


Figure 4: r_m/r_H versus δt . Here we have fixed $r_H = 1$ and $a = 0.45$. The curves obtained for another values of the anisotropy parameter are almost coincident with the above results.

Therefore, the late time behaviour of dI_{WDW}/dt is obtained by taking the limit $r_m \rightarrow r_H$ in the equation (65)

$$\frac{dI_{\text{WDW}}}{dt} = \frac{V_{d-1}}{16\pi G_N} \left[\int_{\epsilon_0}^{r_H} dr \sqrt{G_{tt} G_{rr} G} \mathcal{L}(r) + \sqrt{\frac{G_{tt} G}{G_{rr}}} \left(\frac{\partial_r G_{tt}}{G_{tt}} + \frac{\partial_r G}{G} \right) \Big|_{r=\epsilon_0} + \sqrt{\frac{G}{G_{rr} G_{tt}}} \partial_r G_{tt} \Big|_{r=r_H} \right] \quad (67)$$

Substituting the metric functions $G_{mn}(r)$ and the on-shell Lagrangian $\mathcal{L}(r)$ for the MT model and expanding the above contributions for small anisotropies, we obtain

$$\int_{\epsilon_0}^{r_H} dr \sqrt{G_{tt} G_{rr} G} \mathcal{L}(r) = -2r_H^4 - \frac{5}{6} r_H^2 a^2 \log 2 + \mathcal{O}(\epsilon_0^4 \log \epsilon_0) , \quad (68)$$

$$\sqrt{\frac{G_{tt} G}{G_{rr}}} \left(\frac{\partial_r G_{tt}}{G_{tt}} + \frac{\partial_r G}{G} \right) \Big|_{r=\epsilon_0} = 4r_H^4 + \frac{1}{6} r_H^2 a^2 (10 \log 2 - 1) + \mathcal{O}(\epsilon_0^4 \log \epsilon_0) , \quad (69)$$

$$\sqrt{\frac{G}{G_{rr} G_{tt}}} \partial_r G_{tt} \Big|_{r=r_H} = 4r_H^4 + \frac{1}{3} r_H^2 a^2 (5 \log 2 - 1) . \quad (70)$$

By summing the above contributions and taking the limit $\epsilon_0 \rightarrow 0$ we find

$$\frac{dI_{\text{WDW}}}{dt} = \frac{V_3}{16\pi G_N} \left(6r_H^4 + \frac{r_H^2 a^2}{2} (5 \log(2) - 1) \right) = 2M(a) \quad (71)$$

where the mass of the black brane $M(a)$ is given by equation (13). Therefore, the late time behaviour of the time derivative of holographic complexity reads

$$\frac{d\mathcal{C}_A}{dt} = \frac{2M(a)}{\pi\hbar}, \quad (72)$$

which saturates the Lloyd's bound. We have checked that the same late-time result for $\frac{d\mathcal{C}_A}{dt}$ can be obtained by following the approach developed by Brown et al [7]. See appendix B.

3.2.2 Full time behaviour

In this section we study the full time behaviour of holographic complexity for the MT model. We numerically solve the equation (61) to find r_m as a function of δt and then we use the result in equation (65) to obtain I_{WDW} as a function of δt .

The geometry in the MT model is controlled by the dimensionless parameter ar_H , where a is the parameter of anisotropy. The values of (a, r_H, M) for which we study the complexity growth are shown in table 1, and they were chosen such that the temperature is fixed as we increase the anisotropy. In this table we can see that the black brane's mass increases as we increase a while keeping T fixed. Figure 5 shows the time dependence of the gravitational action in the WDW patch for the choice of parameters presented in table 1. The behaviour of $d\mathcal{C}_A/dt$ is qualitatively similar to behaviour observed in isotropic systems. The anisotropy increase the mass of the black brane and its effects on the rate of change of complexity seem to be just a vertical shift in the curves of $d\mathcal{C}_A/dt$ versus t .

Table 1: black brane's mass, measured in units of $V_3/(16\pi G_N)$, for several values of a and r_H . Here we chosen r_H such that the Hawking temperature is fixed $T = 1/\pi$.

anisotropy parameter	r_H such that $T = 1/\pi$	black brane's mass
$a = 0.00$	$r_H = 1.000000$	$M = 3.00000$
$a = 0.45$	$r_H = 0.993778$	$M = 3.04931$
$a = 0.60$	$r_H = 0.988883$	$M = 3.08582$

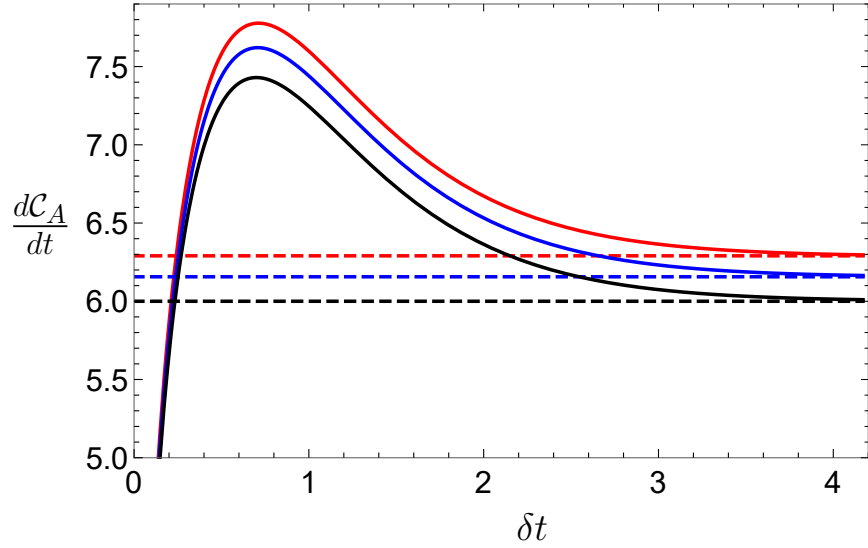


Figure 5: The time dependence of holographic complexity calculated with the CA proposal. The curves correspond to: $(a, r_H, 2M) = (0, 1, 6)$ (black curves), $(a, r_H, 2M) = (0.45, 0.994, 6.10)$ (blue curves) and $(a, r_H, 2M) = (0.6, 0.989, 6.17)$ (red curves). The continuous curves represent the results (in units of $V_3/(16\pi^2 \hbar G_N)$) for the time derivative of holographic complexity, while the dashed horizontal lines represent $2M$. We fix the normalization of the null-vector in equation (52) by taking $\alpha = 1.3$. The qualitative behaviour is the same for other values of α .

4 Discussion

We have used the CA conjecture to study the time-dependence of holographic complexity for an anisotropic black brane solution. The gravitational solution is dual to the $\mathcal{N} = 4$ SYM theory deformed by a position-dependent theta-term that breaks isotropy and conformal invariance. The background geometry is controlled by the ratio a/T , where a is the parameter of anisotropy, and T is the Hawking temperature. In the following we discuss the effects of the anisotropy on the holographic complexity.

Similarly to the case of isotropic systems, the rate of change of complexity in anisotropic systems is zero for $t \leq t_c$, and it is non-zero for $t > t_c$, with this critical time given by equation (24). Figure 3 shows the behaviour of t_c as a function of the anisotropy parameter. In this figure we consider increasing values of the anisotropy parameter, while keeping fixed the temperature. As compared with an isotropic system with the same temperature, the holographic complexity of anisotropic systems remains constant for a shorter period, i.e., the effect of the anisotropy is to reduce t_c .

In section 3.2.1 we study the late-time behaviour of the holographic complexity and find an expression for dI_{WDW}/dt in terms of the metric functions. See equation (67). For simplicity, let us first consider the isotropic case, in which $a = 0$. In this case the MT solution reduces to the five-dimensional black brane solution that is dual to the undeformed $\mathcal{N} = 4$ SYM theory.

From previous works [7, 16, 17], we know that the Lloyd’s bound should be respected in this case. As we turn on a small anisotropy parameter, all the metric functions get corrections up to the second order in a and this leads to a larger black brane’s mass (see equation (13)). In this case, we expect the formula (67) to provide the result for $a = 0$, plus corrections up to the second order in the anisotropy parameter. Applying our formulas for the MT model we find that the late time rate of change of complexity matches the Lloyd’s bound, i.e., $d\mathcal{C}_A/dt = 2M(a)/\pi\hbar$. This is a highly non-trivial match, because it means that the anisotropy increases the value of $2M$ and the late time value of dI_{WDW}/dt precisely in the same amount.

The full-time behaviour of $d\mathcal{C}_A/dt$ can be seen in figure 5. The results share a lot of similarities with the previous results obtained for isotropic systems [16]. In particular, $d\mathcal{C}_A/dt$ violates the Lloyd’s bound at initial times, and approaches this bound (from above) at later times. In this figure we consider increasing values of the anisotropy parameter, while keeping fixed the temperature. The resulting black brane’s mass increases as we increase the anisotropy parameter, and the overall effect of the anisotropy is a vertical upward shift in the curves of $d\mathcal{C}_A/dt$ versus δt . At later times, the difference between the anisotropic and isotropic results is proportional to the difference in pressures in the transverse and longitudinal directions, namely

$$\frac{d\mathcal{C}_A}{dt} = \frac{2M(0)}{\pi\hbar} + \frac{V_3}{\pi\hbar}(P_{xy} - P_z). \quad (73)$$

This can be seen from equations (72) and (14).

Future directions

We have studied the effects of anisotropy on the complexity growth considering the case of small anisotropies. Our results are valid up to $\mathcal{O}(a^2)$. It would be interesting to extend our results to higher anisotropies, because in this case the MT model displays a conformal anomaly⁹, which might cause a violation of the Lloyd’s bound. Besides that, the MT gravitational solution can be thought of as describing a renormalization group (RG) flow from a AdS geometry in the ultraviolet (UV) to a Lifshitz geometry in the infrared (IR). The parameter controlling this transition is the ratio a/T , which is small close to the UV fixed point and large close to the IR fixed point. It would be interesting to study how the complexity growth behaves under this RG flow. Moreover, as Lifshitz geometries were known to violate the Lloyd’s bound [23], we expect such a violation to occur in the MT model at higher anisotropies.

Another interesting extension of this work would be to study the effects of the anisotropy in the holographic complexity calculated using the CV conjecture. Although this calculation is relatively easy for isotropic systems [5, 16, 17], the extension for anisotropic systems is non-trivial, because in this case the ansatz for the maximum volume surface is more complicated, preventing the use of the techniques used in [5, 16, 17].

⁹In the MT model the conformal anomaly appears at order $\mathcal{O}(a^4)$.

Acknowledgments

We are grateful to Hesam Soltanpanahi and Alberto Güijosa for very useful discussions and comments. We also thank Hamid Rajaian and Hugo Marrochio for useful correspondence and for comments on the manuscript. MMQ is supported by Institute for Research in Fundamental Sciences (IPM). VJ and YDO were supported by Mexico's National Council of Science and Technology (CONACyT) grant CB-2014/238734.

A Joint terms at the $r = r_{\max}$ and $r = \epsilon_0$ cutoff surfaces

In this appendix we briefly review how to calculate the joint terms at the asymptotic boundaries and at the singularities. We show that the contributions from the asymptotic boundaries are time-independent, while the contributions from the singularities vanish.

A joint term for a corner involving the connection of at least one null surface has the form [15]

$$I_{\text{joint}} = \frac{1}{8\pi G_N} \int d^{d-1}x \sqrt{\sigma} a \quad (74)$$

where σ is the induced metric on the surfaces and a is defined as

$$a = \pm \begin{cases} \log |k \cdot n^{(t)}| & \text{for spacelike-null joints} \\ \log |k \cdot n^{(s)}| & \text{for timelike-null joints} \\ \log |k^+ \cdot k^- / 2| & \text{for null-null joints} \end{cases}$$

where k^+ and k^- are outward directed null normal vectors, while $n^{(t)}(n^{(s)})$ are outward directed timelike (spacelike) normal vectors. The overall sign depends on the orientation of the normal vectors. For more details, see the appendix A of [15]. The relevant normal vectors can be written as

$$n_\mu^{(t)} = (n_t^{(t)}, n_r^{(t)}, n_i^{(t)}) = (0, \sqrt{-G_{rr}(\epsilon_0)}, 0), \quad (75)$$

$$n_\mu^{(s)} = (n_t^{(s)}, n_r^{(s)}, n_i^{(s)}) = (0, \sqrt{G_{rr}(r_{\max})}, 0), \quad (76)$$

$$k_\mu^\pm = \pm \alpha \partial_\mu(t \pm r^*). \quad (77)$$

With the above definitions, the joints term coming from the singularities can be written as

$$I_{\text{joint}}^{\text{sing}} = \frac{1}{8\pi G_N} \int d^{d-1}x \sqrt{\sigma} \log |k \cdot n^{(t)}| = -\frac{V_{d-1}}{8\pi G_N} G(r) \log |G_{tt}(r)| \Big|_{r=\epsilon_0}. \quad (78)$$

For the MT model, one can show that $I_{\text{joint}}^{\text{sing}} \sim \epsilon_0^3 \log \epsilon_0$. Therefore, the contribution from this joint term vanishes in the limit $\epsilon_0 \rightarrow 0$.

The joint terms coming from the asymptotic boundaries are given by

$$I_{\text{joint}}^{\text{bdry}} = \frac{1}{8\pi G_N} \int d^{d-1}x \sqrt{\sigma} \log |k \cdot n^{(s)}| = \frac{V_{d-1}}{8\pi G_N} G(r) \log |G_{tt}(r)| \Big|_{r=r_{\max}}. \quad (79)$$

For the MT model $I_{\text{joint}}^{\text{bdry}}$ gives rise to a divergent contribution that is independent of time, because it only depends on quantities calculated on the outside of the black brane, and this region has a time-translation symmetry. Therefore, this term do not contribute to the rate of change of holographic complexity.

B Comparison with Brown et al

The CA conjecture was proposed by Brown et al in [6, 7]. In those papers the authors find a clever way of calculating the late time rate of change of complexity without having to take into account the contributions from joint and null boundary terms. In a later work, Myers et al [14] derive the expressions for the joint and null boundary terms and showed how to include the corresponding contributions to the rate of change of holographic complexity. Myers et al find a perfect match with the results of Brown et al at later times and carefully explain the reasons behind the agreement in [14]. In this appendix we briefly review the approach of Brown et al and we show that it gives the same results obtained in section 3 using the approach of Myers et al [14, 15].

In the approach of Brown et al it is more convenient to consider the time evolution of the WDW patch when we increase the time in the left boundary, while keeping fixed the time in the right boundary, as shown in figure 6.

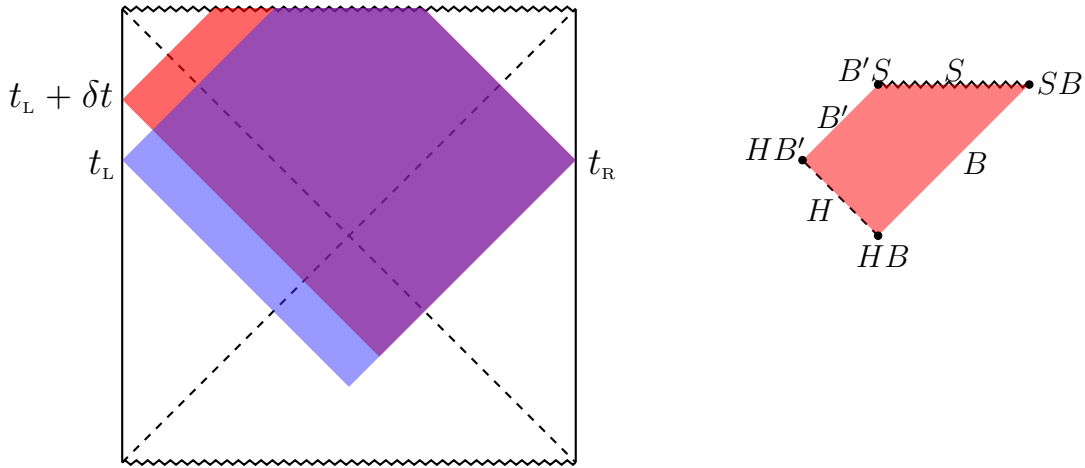


Figure 6: Left panel: change in the WDW patch as the time evolves in the left boundary. Right panel: piece of the WDW patch that contributes to the rate of change of complexity at late times.

The left hand side of figure 6 shows that, as the time evolves in the left boundary, the WDW patch increases in the region shown in red, while it decreases in the region shown in light-blue. To calculate the corresponding variation of the WDW patch, the authors of [7] argue as follows:

- the parts of the WDW patch that lie outside of the horizon are time-independent because this region has a time-translation symmetry. As a consequence, these parts do not contribute to the rate of change of complexity;
- the part of the WDW patch that lies inside the past horizon contributes at early times, but it is highly suppressed at later times. Hence, at later times, the only contribution for the rate of change of complexity comes from the region of the WDW patch that lies inside the future horizon. This region is shown in the right hand side of figure 6;
- under time evolution the surface B is replaced by the surface B' , while the corners HB and SB are replaced by the corners HB' and $S'B$, respectively. The surfaces B and B' are related by a time-translation symmetry and so their contributions cancel. The same cancellation occurs between the contributions coming from HB and HB' and between the contributions coming from SB and $B'S$;

With the above cancellations the only terms left to be computed are the bulk contribution and the surface contributions coming from the horizon H and from the singularity S . Therefore, the gravitational action evaluated in the WDW patch can be written as

$$I_{\text{WDW}} = I_{\text{bulk}} + I_{\text{surface}} , \quad (80)$$

where the bulk contribution reads

$$I_{\text{bulk}} = \frac{1}{16\pi G_{\text{N}}} \int_{\mathcal{M}} d^{d+1}x \sqrt{-g} \mathcal{L}(x) \quad (81)$$

while the GHY surface contribution reads

$$I_{\text{surface}} = \frac{1}{8\pi G_{\text{N}}} \int_{r=r_{\text{H}}} d^d x \sqrt{|h|} K + \frac{1}{8\pi G_{\text{N}}} \int_{r=\epsilon_0} d^d x \sqrt{|h|} K \quad (82)$$

where $r = r_{\text{H}}$ indicates the boundary surface at the horizon and $r = \epsilon_0$ indicates the boundary surface at the singularity.

For the general action and metric given in (15) and (16) we can write

$$\begin{aligned} I_{\text{WDW}} = & \frac{V_{d-1}}{16\pi G_{\text{N}}} \int dt \int_{\epsilon_0}^{r_{\text{H}}} dr \sqrt{G_{tt} G_{rr}} \mathcal{L}(r) \\ & + \frac{V_{d-1}}{16\pi G_{\text{N}}} \int dt \left(\sqrt{\frac{G_{tt} G}{G_{rr}}} \left(\frac{\partial_r G_{tt}}{G_{tt}} + \frac{\partial_r G}{G} \right) \Big|_{r=r_{\text{H}}} + \sqrt{\frac{G_{tt} G}{G_{rr}}} \left(\frac{\partial_r G_{tt}}{G_{tt}} + \frac{\partial_r G}{G} \right) \Big|_{r=\epsilon_0} \right) , \end{aligned} \quad (83)$$

where we have used (33) to express K in terms of the metric functions. The time-derivative reads

$$\frac{dI_{\text{WDW}}}{dt} = \frac{V_{d-1}}{16\pi G_{\text{N}}} \left[\int_{\epsilon_0}^{r_{\text{H}}} dr \sqrt{G_{tt} G_{rr}} \mathcal{L}(r) + \sqrt{\frac{G}{G_{tt} G_{rr}}} \partial_r G_{tt} \Big|_{r=r_{\text{H}}} + \sqrt{\frac{G_{tt} G}{G_{rr}}} \left(\frac{\partial_r G_{tt}}{G_{tt}} + \frac{\partial_r G}{G} \right) \Big|_{r=\epsilon_0} \right] , \quad (84)$$

where we have used that G_{tt}/G_{rr} vanishes at the horizon to simplify the expression for the GHY term at the horizon. The above results for the late-time rate of change of I_{WDW} precisely coincides with the result (67) obtained with the approach of Myers et al [14, 15]. The reason

for the agreement is the following: both approaches contain identical bulk contributions and identical surface contributions coming from the future singularity. The only difference is that in the calculation of Brown et al there is a GHY-like term for the horizon, while in the calculation of Myers et al there is no such term, but there is instead a joint contribution coming from a corner that lies just behind the past horizon. Surprisingly, these two terms precisely coincides and both approaches give the same result. A more detailed explanation for the agreement between the two approaches can be found in [14].

References

- [1] J. M. Maldacena, “The large N limit of superconformal field theories and supergravity,” Adv. Theor. Math. Phys. **2**, 231 (1998) [Int. J. Theor. Phys. **38**, 1113 (1999)] [hep-th/9711200].
- [2] S. S. Gubser, I. R. Klebanov, A. M. Polyakov, “Gauge theory correlators from noncritical string theory,” Phys. Lett. **B428**, 105-114 (1998) [hep-th/9802109].
- [3] E. Witten, “Anti-de Sitter space and holography,” Adv. Theor. Math. Phys. **2**, 253-291 (1998) [hep-th/9802150].
- [4] L. Susskind, “Computational Complexity and Black Hole Horizons,” [Fortsch. Phys. **64**, 24 (2016)] Addendum: Fortsch. Phys. **64**, 44 (2016) doi:10.1002/prop.201500093, 10.1002/prop.201500092 [arXiv:1403.5695 [hep-th], arXiv:1402.5674 [hep-th]].
- [5] D. Stanford and L. Susskind, “Complexity and Shock Wave Geometries,” Phys. Rev. D **90**, no. 12, 126007 (2014) doi:10.1103/PhysRevD.90.126007 [arXiv:1406.2678 [hep-th]].
- [6] A. R. Brown, D. A. Roberts, L. Susskind, B. Swingle and Y. Zhao, “Holographic Complexity Equals Bulk Action?,” Phys. Rev. Lett. **116**, no. 19, 191301 (2016) doi:10.1103/PhysRevLett.116.191301 [arXiv:1509.07876 [hep-th]].
- [7] A. R. Brown, D. A. Roberts, L. Susskind, B. Swingle and Y. Zhao, “Complexity, action, and black holes,” Phys. Rev. D **93**, no. 8, 086006 (2016) doi:10.1103/PhysRevD.93.086006 [arXiv:1512.04993 [hep-th]].
- [8] B. Swingle, “Entanglement Renormalization and Holography,” Phys. Rev. D **86**, 065007 (2012) doi:10.1103/PhysRevD.86.065007 [arXiv:0905.1317 [cond-mat.str-el]].
- [9] G. Vidal, “Entanglement Renormalization,” Phys. Rev. Lett. **99**, no. 22, 220405 (2007) doi:10.1103/PhysRevLett.99.220405 [cond-mat/0512165].
- [10] T. Hartman and J. Maldacena, “Time Evolution of Entanglement Entropy from Black Hole Interiors,” JHEP **1305**, 014 (2013) doi:10.1007/JHEP05(2013)014 [arXiv:1303.1080 [hep-th]].
- [11] S. Aaronson, “The Complexity of Quantum States and Transformations: From Quantum Money to Black Holes,” arXiv:1607.05256 [quant-ph].

- [12] J. M. Maldacena, “Eternal black holes in anti-de Sitter,” JHEP **0304**, 021 (2003) [hep-th/0106112].
- [13] S. Lloyd, “Ultimate physical limits to computation,” Nature 406 (2000), no. 6799 10471054 [arXiv:9908043[quant-ph]]
- [14] L. Lehner, R. C. Myers, E. Poisson and R. D. Sorkin, “Gravitational action with null boundaries,” Phys. Rev. D **94**, no. 8, 084046 (2016) doi:10.1103/PhysRevD.94.084046 [arXiv:1609.00207 [hep-th]].
- [15] D. Carmi, R. C. Myers and P. Rath, “Comments on Holographic Complexity,” JHEP **1703**, 118 (2017) doi:10.1007/JHEP03(2017)118 [arXiv:1612.00433 [hep-th]].
- [16] D. Carmi, S. Chapman, H. Marrochio, R. C. Myers and S. Sugishita, “On the Time Dependence of Holographic Complexity,” JHEP **1711**, 188 (2017) doi:10.1007/JHEP11(2017)188 [arXiv:1709.10184 [hep-th]].
- [17] K. Y. Kim, C. Niu, R. Q. Yang and C. Y. Zhang, “Comparison of holographic and field theoretic complexities by time dependent thermofield double states,” arXiv:1710.00600 [hep-th].
- [18] R. Jefferson and R. C. Myers, “Circuit complexity in quantum field theory,” JHEP **1710**, 107 (2017) doi:10.1007/JHEP10(2017)107 [arXiv:1707.08570 [hep-th]].
- [19] S. Chapman, M. P. Heller, H. Marrochio and F. Pastawski, “Toward a Definition of Complexity for Quantum Field Theory States,” Phys. Rev. Lett. **120**, no. 12, 121602 (2018) doi:10.1103/PhysRevLett.120.121602 [arXiv:1707.08582 [hep-th]].
- [20] J. Couch, S. Eccles, W. Fischler and M. L. Xiao, “Holographic complexity and non-commutative gauge theory,” JHEP **1803**, 108 (2018) doi:10.1007/JHEP03(2018)108 [arXiv:1710.07833 [hep-th]].
- [21] M. Alishahiha, A. Faraji Astaneh, M. R. Mohammadi Mozaffar and A. Molabashi, “Complexity Growth with Lifshitz Scaling and Hyperscaling Violation,” arXiv:1802.06740 [hep-th].
- [22] B. Swingle and Y. Wang, “Holographic Complexity of Einstein-Maxwell-Dilaton Gravity,” arXiv:1712.09826 [hep-th].
- [23] Y. S. An and R. H. Peng, “The effect of Dilaton on the holographic complexity growth,” arXiv:1801.03638 [hep-th].
- [24] D. Mateos and D. Trancanelli, “The anisotropic N=4 super Yang-Mills plasma and its instabilities,” Phys. Rev. Lett. **107**, 101601 (2011) [arXiv:1105.3472 [hep-th]].
- [25] D. Mateos and D. Trancanelli, “Thermodynamics and Instabilities of a Strongly Coupled Anisotropic Plasma,” JHEP **1107**, 054 (2011) [arXiv:1106.1637 [hep-th]].
- [26] M. Alishahiha, “Holographic Complexity,” Phys. Rev. D **92**, no. 12, 126009 (2015) doi:10.1103/PhysRevD.92.126009 [arXiv:1509.06614 [hep-th]].

- [27] M. Alishahiha, A. Faraji Astaneh, A. Naseh and M. H. Vahidinia, “On complexity for $F(R)$ and critical gravity,” JHEP **1705**, 009 (2017) doi:10.1007/JHEP05(2017)009 [arXiv:1702.06796 [hep-th]].
- [28] M. Alishahiha and A. Faraji Astaneh, “Holographic Fidelity Susceptibility,” Phys. Rev. D **96**, no. 8, 086004 (2017) doi:10.1103/PhysRevD.96.086004 [arXiv:1705.01834 [hep-th]].
- [29] J. Couch, W. Fischler and P. H. Nguyen, “Noether charge, black hole volume, and complexity,” JHEP **1703**, 119 (2017) doi:10.1007/JHEP03(2017)119 [arXiv:1610.02038 [hep-th]].
- [30] S. Chapman, H. Marrochio and R. C. Myers, “Complexity of Formation in Holography,” JHEP **1701**, 062 (2017) doi:10.1007/JHEP01(2017)062 [arXiv:1610.08063 [hep-th]].
- [31] R. G. Cai, S. M. Ruan, S. J. Wang, R. Q. Yang and R. H. Peng, “Action growth for AdS black holes,” JHEP **1609**, 161 (2016) doi:10.1007/JHEP09(2016)161 [arXiv:1606.08307 [gr-qc]].
- [32] A. R. Brown, L. Susskind and Y. Zhao, “Quantum Complexity and Negative Curvature,” Phys. Rev. D **95**, no. 4, 045010 (2017) doi:10.1103/PhysRevD.95.045010 [arXiv:1608.02612 [hep-th]].
- [33] A. R. Brown and L. Susskind, “The Second Law of Quantum Complexity,” arXiv:1701.01107 [hep-th].
- [34] W. J. Pan and Y. C. Huang, “Holographic complexity and action growth in massive gravities,” Phys. Rev. D **95**, no. 12, 126013 (2017) doi:10.1103/PhysRevD.95.126013 [arXiv:1612.03627 [hep-th]].
- [35] R. Q. Yang, “Strong energy condition and complexity growth bound in holography,” Phys. Rev. D **95**, no. 8, 086017 (2017) doi:10.1103/PhysRevD.95.086017 [arXiv:1610.05090 [gr-qc]].
- [36] D. Momeni, S. A. H. Mansoori and R. Myrzakulov, “Holographic Complexity in Gauge/String Superconductors,” Phys. Lett. B **756**, 354 (2016) doi:10.1016/j.physletb.2016.03.031 [arXiv:1601.03011 [hep-th]].
- [37] D. Momeni, M. Faizal, S. Bahamonde and R. Myrzakulov, “Holographic complexity for time-dependent backgrounds,” Phys. Lett. B **762**, 276 (2016) doi:10.1016/j.physletb.2016.09.036 [arXiv:1610.01542 [hep-th]].
- [38] R. Q. Yang, C. Niu and K. Y. Kim, “Surface Counterterms and Regularized Holographic Complexity,” JHEP **1709**, 042 (2017) doi:10.1007/JHEP09(2017)042 [arXiv:1701.03706 [hep-th]].
- [39] R. G. Cai, M. Sasaki and S. J. Wang, “Action growth of charged black holes with a single horizon,” Phys. Rev. D **95**, no. 12, 124002 (2017) doi:10.1103/PhysRevD.95.124002 [arXiv:1702.06766 [gr-qc]].
- [40] E. Bakhshaei, A. Mollabashi and A. Shirzad, “Holographic Subregion Complexity for Singular Surfaces,” Eur. Phys. J. C **77**, no. 10, 665 (2017) doi:10.1140/epjc/s10052-017-5247-1 [arXiv:1703.03469 [hep-th]].

- [41] F. J. G. Abad, M. Kulaxizi and A. Parnachev, “On Complexity of Holographic Flavors,” arXiv:1705.08424 [hep-th].
- [42] J. Tao, P. Wang and H. Yang, “Testing Holographic Conjectures of Complexity with Born-Infeld Black Holes,” arXiv:1703.06297 [hep-th].
- [43] W. D. Guo, S. W. Wei, Y. Y. Li and Y. X. Liu, “Complexity growth rates for AdS black holes in massive gravity and $f(R)$ gravity,” arXiv:1703.10468 [gr-qc].
- [44] K. Nagasaki, “Complexity of AdS_5 black holes with a rotating string,” arXiv:1707.08376 [hep-th].
- [45] Y. G. Miao and L. Zhao, “Complexity/Action duality of shock wave geometry in a massive gravity theory,” Phys. Rev. D **97**, no. 2, 024035 (2018) doi:10.1103/PhysRevD.97.024035 [arXiv:1708.01779 [hep-th]].
- [46] M. M. Qaemmaqami, “Complexity growth in minimal massive 3D gravity,” Phys. Rev. D **97**, no. 2, 026006 (2018) doi:10.1103/PhysRevD.97.026006 [arXiv:1709.05894 [hep-th]].
- [47] L. Sebastiani, L. Vanzo and S. Zerbini, “Action growth for black holes in modified gravity,” arXiv:1710.05686 [hep-th].
- [48] W. Cottrell and M. Montero, “Complexity is Simple,” arXiv:1710.01175 [hep-th].
- [49] M. Moosa, “Evolution of Complexity Following a Global Quench,” arXiv:1711.02668 [hep-th].
- [50] S. A. Hosseini Mansoori and M. M. Qaemmaqami, “Complexity Growth, Butterfly Velocity and Black hole Thermodynamics,” arXiv:1711.09749 [hep-th].
- [51] X. H. Ge, S. J. Sin, Y. Tian, S. F. Wu and S. Y. Wu, “Charged BTZ-like black hole solutions and the diffusivity-butterfly velocity relation,” arXiv:1712.00705 [hep-th].
- [52] S. J. Zhang, “Complexity and phase transitions in a holographic QCD model,” arXiv:1712.07583 [hep-th].
- [53] M. Moosa, “Divergences in the rate of complexification,” arXiv:1712.07137 [hep-th].
- [54] A. Ovgun and K. Jusufi, “Complexity growth rates for AdS black holes with dyonic/nonlinear charge/ stringy hair/ topological defects,” arXiv:1801.09615 [gr-qc].
- [55] C. A. Agon, M. Headrick and B. Swingle, “Subsystem Complexity and Holography,” arXiv:1804.01561 [hep-th].
- [56] R. Auzzi, S. Baiguera and G. Nardelli, “Volume and complexity for warped AdS black holes,” arXiv:1804.07521 [hep-th].
- [57] Y. S. An, R. G. Cai and Y. Peng, “Time Dependence of Holographic Complexity in Gauss-Bonnet Gravity,” arXiv:1805.07775 [hep-th].
- [58] K. Bamba, D. Momeni and M. A. Ajmi, “Holographic Entanglement Entropy, Complexity, Fidelity Susceptibility and Hierarchical UV/IR Mixing Problem in AdS_2 /open strings,” Int. J. Mod. Phys. A **33**, 1850100 (2018) doi:10.1142/S0217751X18501002 [arXiv:1806.02209 [hep-th]].

- [59] H. Ghaffarnejad, E. Yaraie and M. Farsam, “Complexity growth and shock wave geometry in AdS-Maxwell-power-Yang-Mills theory,” arXiv:1806.07242 [gr-qc].
- [60] H. Ghaffarnejad, M. Farsam and E. Yaraie, “Effects of quintessence dark energy on the action growth and butterfly velocity,” arXiv:1806.05735 [hep-th].
- [61] R. Auzzi, S. Baiguera, M. Grassi, G. Nardelli and N. Zenoni, “Complexity and action for warped AdS black holes,” arXiv:1806.06216 [hep-th].
- [62] R. Fareghbal and P. Karimi, “Complexity Growth in Flatland,” arXiv:1806.07273 [hep-th].
- [63] K. Nagasaki, “Complexity growth of rotating black holes with a probe string,” arXiv:1807.01088 [hep-th].
- [64] J. Casalderrey-Solana, H. Liu, D. Mateos, K. Rajagopal and U. A. Wiedemann, “Gauge/String Duality, Hot QCD and Heavy Ion Collisions,” book:Gauge/String Duality, Hot QCD and Heavy Ion Collisions. Cambridge, UK: Cambridge University Press, 2014 doi:10.1017/CBO9781139136747 [arXiv:1101.0618 [hep-th]].
- [65] L. Cheng, X. H. Ge and S. J. Sin, “Anisotropic plasma at finite $U(1)$ chemical potential,” JHEP **1407**, 083 (2014) doi:10.1007/JHEP07(2014)083 [arXiv:1404.5027 [hep-th]].
- [66] V. Jahnke, A. S. Misobuchi and D. Trancanelli, “Holographic renormalization and anisotropic black branes in higher curvature gravity,” JHEP **1501**, 122 (2015) doi:10.1007/JHEP01(2015)122 [arXiv:1411.5964 [hep-th]].
- [67] J.W. York, Jr., “Role of conformal three geometry in the dynamics of gravitation,” Phys. Rev. Lett. **28** (1972) 1082.
- [68] G.W. Gibbons, S. W. Hawking, “Action Integrals and Partition Functions in Quantum Gravity,” Phys. Rev. D **15** (1977) 2752.
- [69] G. Hayward, “Gravitational action for space-times with nonsmooth boundaries,” Phys. Rev. D **47** (1993) 3275.
- [70] D. Brill and G. Hayward, “Is the gravitational action additive?,” Phys. Rev. D **50**, 4914 (1994) doi:10.1103/PhysRevD.50.4914 [gr-qc/9403018].